Journal of Food Process Engineering

Journal of Food Process Engineering ISSN 1745-4530

BARRIER PROPERTIES AND MICROSTRUCTURE OF PULLULAN–ALGINATE-BASED FILMS

QIAN XIAO[1,5], KUN LU[2], QUNYI TONG[3] and CHANG LIU[4]

[1]School of Food Science and Technology, Hunan Agriculture University, Changsha, Hunan 410128, China
[2]SIPO, Patent Examination Cooperation Jiangsu Centre, Suzhou, Jiangsu, China
[3]State Key Laboratory of Food Science and Technology, Jiangnan University, Wuxi, Jiangsu, China
[4]Hsingwu Business and Tourism School, Shanghai Lida Polytechnic Institute, Shanghai, China

[5]Corresponding author.
TEL: +86-0731-84617013;
FAX: +86-0731-84617013;
EMAIL: baby.qianxiao@gmail.com

Received for Publication May 28, 2014
Accepted for Publication August 15, 2014

doi:10.1111/jfpe.12151

ABSTRACT

In this study, the barrier properties, crystalline structure and morphology of pullulan–sodium alginate-based films were investigated. Among the tested samples, pure pullulan films exhibited the lowest water vapor permeability and oxygen permeability values (7.053×10^{-6} g.m/Pa.h.m^2 and 0.48x10^{-6} mL.mm/m^{2}day.pa, respectively). Incorporating pullulan into alginate, the absorbance bands of COO^- groups shifted significantly to higher wavenumbers (1,640 and 1,413 cm^{-1}, respectively). This could be attributed to the disruption of intermolecular hydrogen bonds present originally between the carboxylic groups caused by added pullulan. The diffractogram of pullulan films indicated that pullulan was a fully amorphous polymer, whereas that of sodium alginate exhibited semi-crystalline features. Furthermore, the morphology of pullulan–alginate-based film was studied by atomic force microscopy. Roughness parameter (R_q and R_a) values increased significantly with the incorporation of alginate content into pullulan.

PRACTICAL APPLICATIONS

Because pure pullulan, alginate and their blend film are highly water soluble, transparent, tasteless, odorless and heat sealable and poses low permeability to oxygen, they could potentially be a secondary packaging material for beverage products such as instant coffees and cocoa.

INTRODUCTION

Edible films have emerged as an alternative to synthetic plastics for food packaging because they are versatile, renewable and biodegradable (Siew *et al.* 1999). Edible films can prevent quality deterioration and prolong the shelf life of food products because of their selective barrier properties against the migration of moisture, gases and vapor (Giancone *et al.* 2008). A variety of biopolymers, including polysaccharides, proteins, lipids and their combination, can be used as film-forming materials to prepare edible films (Gennadios *et al.* 1996). Widespread works have been performed to study the properties and applications of combination films, as these can potentially enhance material properties.

Pullulan is an extracellular water-soluble microbial polysaccharide produced by *Aureobasidium pullulans* in starch and sugar cultures. The linear polymer mainly consists of maltotriose units interconnected to each other by α-(1, 6) glycosidic bonds. This unique linkage pattern endows pullulan with distinctive physical properties to form a film that is strong, transparent and water soluble, and with low permeability to oil and oxygen (Singh *et al.* 2008). Alginate, a linear polysaccharide extracted from brown seaweed, is composed of variable proportions of β-D-mannuronic acid (M-block) and α-L-guluronic acid (G-block) linked by 1-4 glycosidic bonds. The block copolymer consisted of homopolymeric regions of M- and G-blocks, separated by regions that contain M and G units (Fu *et al.* 2011). The proportion and distribution of these blocks determine the physicochemical properties of the biopolymer (Lacroix and Le Tien 2005). Sodium alginate is a polyelectrolyte with negative charges on its backbone (Zhong *et al.* 2010). It dissolves readily in water to form a homogeneous film-forming solution, which upon drying, can yield coherent films that have a wide range of food and nonfood applications (Skjak-Bræk *et al.* 2006).

Several researchers have studied the basic properties of pullulan- or alginate-based films. Shih *et al.* (2011) reported that water vapor barrier properties of pullulan films were improved with increased addition of rice wax. The Yong's modulus and tensile strength increased significantly by adding nanofibibrillated cellulose content (Trovatti *et al.* 2012). Incorporating gelatin to pullulan, the oxygen permeability of resulting films is reduced. However, the opposite trend has been observed for their mechanical properties (Zhang *et al.* 2013). For alginate-based films, higher tensile strength, higher Yong's modulus and lower water vapor barrier property were favoured by higher immersion times in CaCl2 and lower cashew tree gum (Azeredo, *et al.*, 2012). Water vapor permeability (WVP) of alginate–pectin films increased gradually with increasing pectin content (Galus and Lenart 2013). Sirvio *et al.* (2014) also reported that the tensile strength of alginate-based films increased, obviously, through incorporation of nanofibrillated cellulose.

In our previous study, we observed the mechanical and thermal properties of pullulan–alginate-based films (Xiao *et al.* 2012). However, barrier properties, crystalline structure and morphology have not been investigated. The objective of this article was to characterize the water vapor and oxygen permeability, microstructure of pullulan, alginate and blend films.

MATERIALS AND METHODS

Materials

Pullulan PI20 (MW 200,000 Da) was donated by Hayashibara Biochemical Lab, Inc. (Shanghai, China). Sodium alginate was obtained from Sigma-Aldrich Co. China (Shanghai, China).

Film Preparation

Pullulan and sodium alginate powders were mixed at three pullulan : alginate weight ratios (100:0, 60:40 and 0:100), dispersed in distilled water and mixed for 3 h under 1,300 rpm by a magnetic stirrer to form a homogeneous film-forming solution. The film-forming solutions were then casted on leveled glass plates and allowed to dry in an environmental chamber maintained at 50°C and 55% RH. The resulting films were peeled off from the glass plates and further conditioned at 23°C and 55% RH prior to testing.

Film Thickness Measurements

Film thickness was measured with a digital micrometer (DELI Testing Machines, Inc., Beijing, China). Measurements of one film sample were taken at five different positions, and the average value was calculated.

WVP

The WVP of the film specimens was measured according to the modified ASTM E96-00 method (ASTM 1993). Glass cups with a 3-cm diameter and 4-cm depth were used. To maintain 55% RH in the cup headspace, 3 g of dried $CaCl_2$ was added into the cup. The rim of the cup is then sealed using the film by applying molten paraffin. The cups were placed in hermetically sealed jars maintained at 23°C and 55% RH. The amount of water that permeated through the films was determined from the weight gain of the cups. WVP was calculated using the following equation.

$$WVP = \frac{\Delta w}{\Delta t \times A} \times \frac{L}{\Delta p} \tag{1}$$

where $\Delta w/\Delta t$ is the rate of water gain, g/h; A is the exposed area of the film, m^2; L is the mean thickness of film specimens, m; and Δp is the difference in partial water vapor pressure between the two sides of film specimens.

Oxygen Permeability

An Ox-Tran 2/20 permeability tester (Mocon, Inc., Minneapolis, MN) was used to determine the oxygen transmission rate (OTR, mL/m^2.day) of pullulan-based films at 23°C and $55 \pm 1\%$ RH, according to the ASTM D3985 (ASTM 1995). A stainless steel mask with 5 cm^2 of open testing area was used to reduce oxygen transfer in a film. One side of the film was exposed to nitrogen gas (98% nitrogen and 2% hydrogen) flow and the other side was exposed to 100% oxygen gas flow. Oxygen permeability coefficients, Po_2 (mL.mm/m^2.day.pa), were calculated by multiplying OTR with film thickness and dividing by Δp.

Fourier Transform Infrared Spectroscopy

Fourier transform infrared spectroscopy (FTIR) spectra of film specimens were determined in attenuated total reflection (ATR) mode using an FTIR spectrometer (IRPrestige-21, Shimadzu Corporation, Tokyo, Japan). All spectra were collected at 23°C from 4,000 to 700 cm^{-1} with a resolution of 4 cm^{-1} at an average of 32 scans. Baseline correction was done using Grams-32 spectral analysis software (Galactic Industries Corp., Salem, NH).

X-Ray Diffraction

The structural properties of films were characterized by a Rigaku D/MAX-RB X-ray diffractometer (Rigaku, Tokyo, Japan, 40 kV, 50 mA) equipped with Cu Kα radiation ($\lambda = 0.1542$ nm). The scan data were collected in the 2θ range from 5° to 40° at 10° min^{-1} scan rate.

Atomic Force Microscopy

Before testing, samples were preconditioned at 55% RH and at room temperature for at least 48 h. The surface morphology of the films was analyzed using an atomic force microscope CSPM 4000 (Benyuan, Inc., Beijing, China). Square filmstrips with dimensions of 2.5×2.5 mm^2 were fixed on mica disks using double-sided tapes. Atomic force microscopy (AFM) photos ($3,000 \times 3,000$ nm) of the films were obtained using the contact mode on their air side. Surface roughness parameters (R_q and R_a) of the films were calculated using the CSPM imager software (version 4.60).

Statistical Analysis

All experiments were conducted in triplicate. Nonlinear regression procedure (PROC NLIN) and analysis of variance procedures were adopted to analyze the data, using SAS software (Statistical Analysis System Institute, Inc., Cary, NC).

RESULTS

Barrier Properties

The WVP data for pure pullulan, alginate and blend films are summarized in Fig. 1a. As shown, pullulan films exhibited lower WVP value (7.053×10^{-6}, g.m/Pa.h.m^2) compared with alginate films (25.745×10^{-6}, g.m/Pa.h.m^2). This could be attributed to the difference of molecular structure between pullulan and sodium alginate. Alginate was more hydrophilic than pullulan because of the substituted hydrophilic group $-COO^{-}Na^{+}$ for alginate. Note that the WVP value of 60:40 pullulan : alginate blend films (16.005×10^{-6} g.m/Pa.h.m^2) was significantly higher than that of pure pullulan films (Fig. 1a). Adding alginate to pullulan films led to interactions between pullulan and alginate, which disrupted the hydrogen bonding network of pure pullulan molecules. In addition, the affinity for water molecules of blend films would be stronger than that of pure pullulan films, as alginate was more hygroscopic compared with pullulan. In Fig. 1b, the oxygen permeability coefficients (Po_2) of pullulan, alginate and blend films are presented. The Po_2 of pullulan films was 0.48×10^{-6} mL.mm/m^2.day.pa, which was significantly lower than that of pure alginate films (8.94×10^{-6} mL.mm/m^2.day.pa). Rojas-Grau *et al.* (2007) also observed that the Po_2 value of pure alginate films was 10.2×10^{-6} mL.mm/m^2.day.pa (which was slightly higher than our results). Moreover, the Po_2 value of 60:40 pullulan : alginate films was nearly four times less in magnitude than that of pure alginate films. This result followed a similar trend as WVP data. And it indicated that interactions formed between pullulan chains and alginate chains, when incorporating alginate into pullulan-based films.

FTIR Analysis

Figure 2a shows the ATR-FTIR spectra in the range of 1,800–940 cm^{-1} for pullulan, alginate and blend films. For alginate films, the absorbance band around 1,593 and 1,406 cm^{-1} were assigned to antisymmetric and symmetric

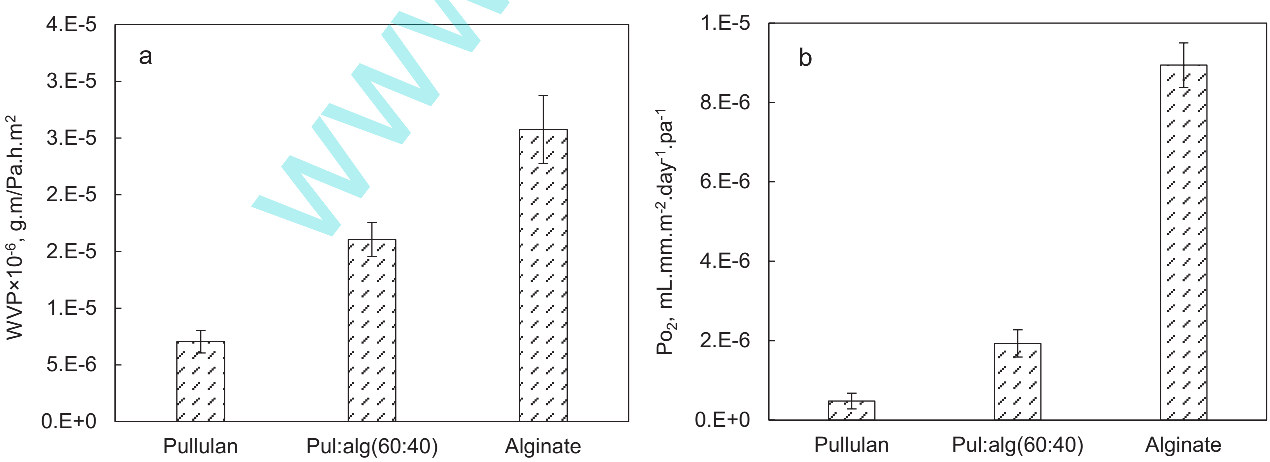

FIG. 1. (A) WATER VAPOR PERMEABILITY, AND (B) OXYGEN PERMEABILITY COEFFICIENTS OF PULLULAN, ALGINATE AND BLEND FILMS AT 23C AND 55% RELATIVE HUMIDITY (RH)
For each measurement, three replicates of three film types were tested.

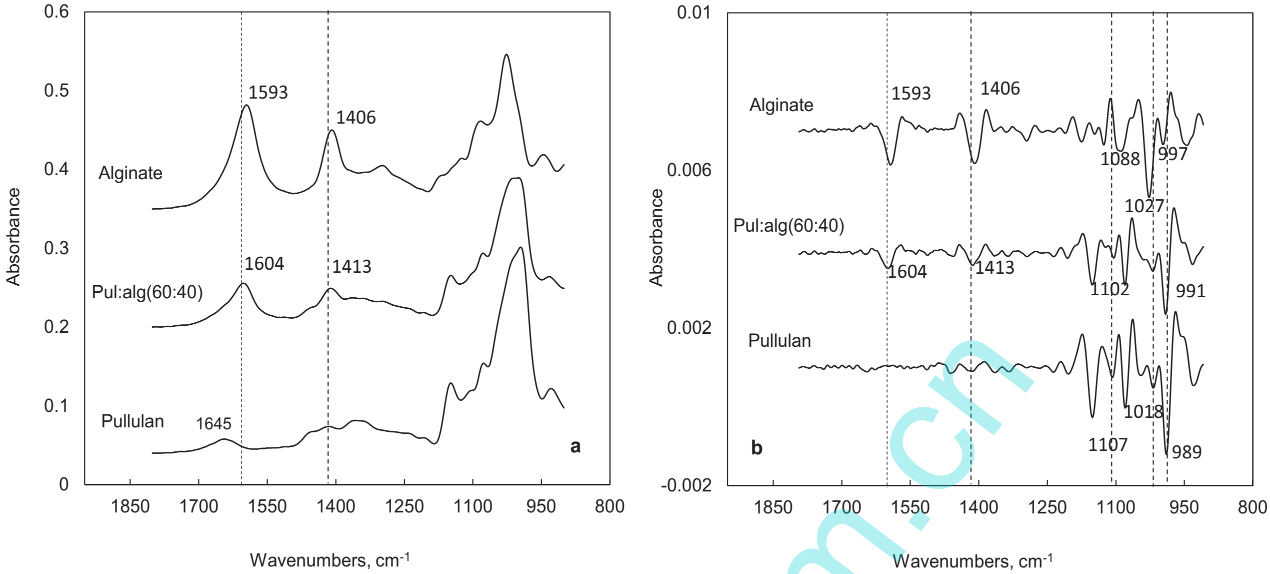

FIG. 2. (A) ORIGIN ATTENUATED TOTAL REFLECTION–FOURIER TRANSFORM INFRARED SPECTRA, (B) SECOND DERIVATIVE SPECTRA IN THE RANGE OF 1,800–940 CM^{-1} FOR PULLULAN, ALGINATE AND BLEND FILMS AT 23 ± 1C AND 55 ± 1% RH
For each measurement, three replicates of three film types were tested.

stretching vibrations of COO$^-$ groups, respectively (Caykara *et al.* 2005; Leal *et al.* 2008; Salomonsen *et al.* 2008). Incorporating pullulan into alginate, the absorbance bands of COO$^-$ groups significantly shifted to higher wavenumbers (1,640 and 1,413 cm^{-1}, respectively). This could be attributed to the disruption of intermolecular hydrogen bonds originally present between the carboxylic groups caused by added pullulan. As shown in Fig. 2a, the 1,060–940 cm^{-1} region of the spectra exhibited many overlapping bands. To facilitate the analysis of frequency shift for the constituted bands, second derivative was applied to this region (Fig. 2b). Absorbance band around 1,107 cm^{-1} of pullulan spectrum was associated with the vibration of the C–O bond at the C_4 position of a glucose residue (Shingel 2002; Sakata and Otsuka 2009). Adding alginate caused the C–O band shifted to 1,102 cm^{-1}, which indicated that oxygen atoms at the fourth of the glucose residue for pullulan molecular were likely involved in hydrogen bonding with alginate. For pure alginate, absorbance band around 1,028 cm^{-1} was attributed to the O–H bending vibration of alginate (Leal *et al.* 2008; Gomez-Ordoñez and Ruperez 2011). Note that the position of this band shifted to a lower wavenumber (1,076 cm^{-1}) with alginate added in. This observation indicated that oxygen atoms at the second and third positions of the six-membered (pyranose) ring for alginate might have hydrogen bonded with pullulan chains.

X-Ray Diffraction Analysis

The X-ray diffraction (XRD) patterns of pullulan, alginate and blend films are presented in Fig. 3. The diffractogram of pullulan films showed a weak broad peak centered at $2\theta = 19°$, indicating that pullulan was a fully amorphous polymer. Similar results have been reported by Trovatti *et al.* (2012) and Zhang *et al.* (2013). However, a diffractogram of alginate films consisted of a board band at $2\theta = 15°$ and a sharp peak at around $2\theta = 22.5°$, corresponding to the amorphous and crystalline regions of alginate, respectively. Similar diffractograms for alginate have been reported (Yang *et al.* 2000; Li *et al.* 2011; Huq *et al.* 2012). Compared

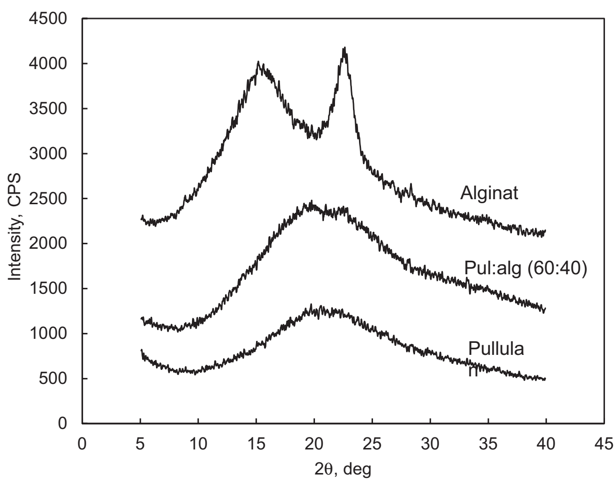

FIG. 3. X-RAY PATTERNS OF PULLULAN, ALGINATE AND BLEND FILMS AT 23 ± 1C AND 55 ± 1% RH
For each measurement, three replicates of three film types were tested.

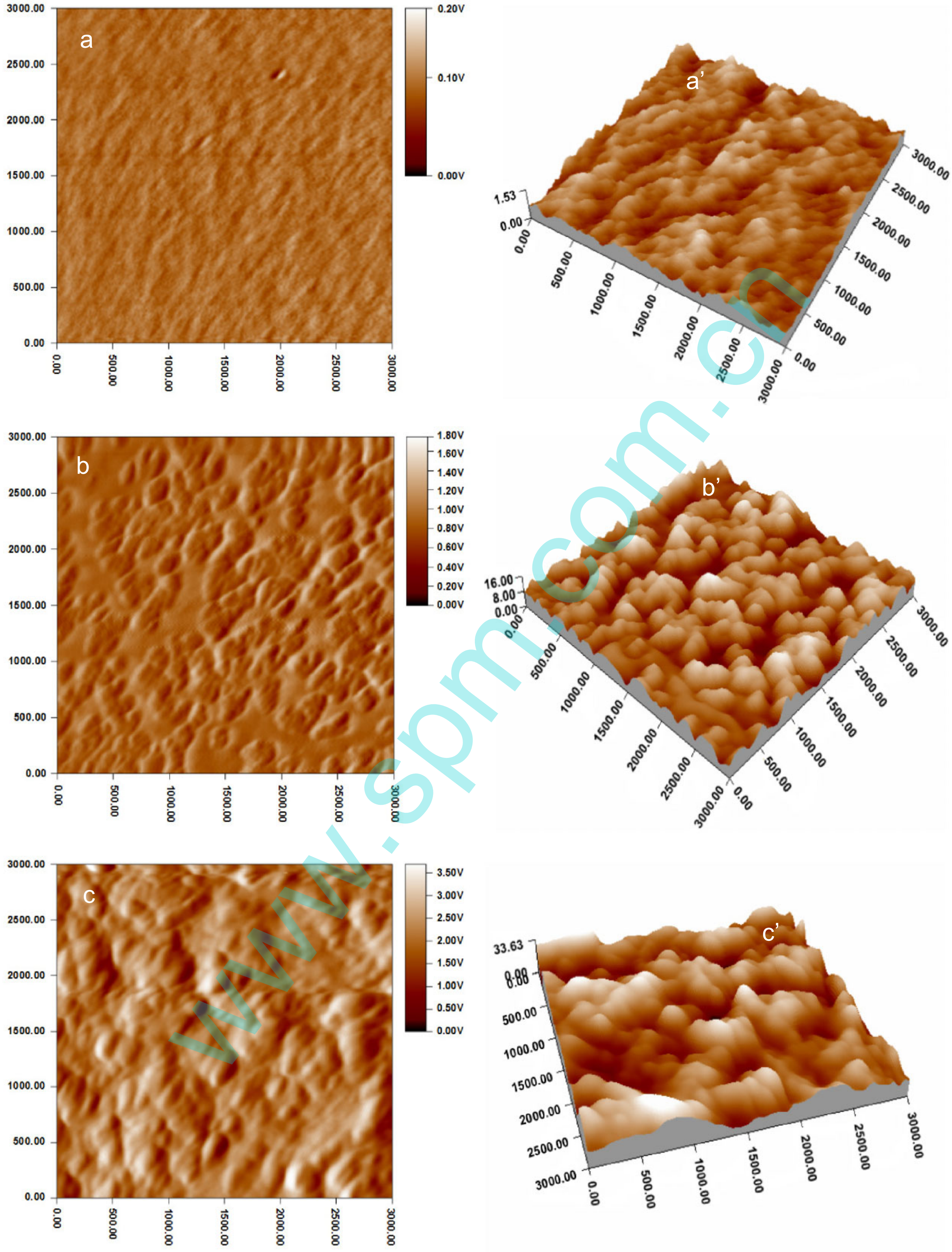

FIG. 4. ATOMIC FORCE MICROSCOPY IMAGES OF PULLULAN–ALGINATE-BASED FILMS AT 23 ± 1C AND 55 ± 1% RH
(a) Height image of pullulan; (b) height image of blend films; (c) height image of pure alginate; (a′) 3-D image of pullulan; (b′) 3-D image of blend films; and (c′) 3-D image of pure alginate.

with pure pullulan films, the board peak at $2\theta = 19°$ of pullulan/alginate blend films shifted to a higher degree ($2\theta = 21°$), and its intensity was enhanced. Moreover, the characteristic peak of alginate at $2\theta = 22.5°$ disappeared for the pullulan/alginate blend films. These observations indicated that strong interactions occurred between pullulan and alginate, when incorporating alginate into pullulan. This is consistent with the results of oxygen permeability tests for pullulan–alginate blend films (Fig. 1b).

AFM

The surface structure of pullulan, alginate and blend films was analyzed by AFM. This technique has been used previously in edible films (Fabra *et al.* 2009). As shown in Fig. 4a,c, the pullulan films exhibited a smooth morphology with very small dust particles, while pure alginate displayed a textured surface consisting of packed grain-like particles. Incorporating alginate into pullulan distinctly changed the surface topographies of the resulting films, which showed the apparent peaks and valley interlacements in the surface (Fig. 4b). Roughness parameters (R_q and R_a) were calculated using the CSPM imager software to quantitatively reflect the alteration in surface topographies of the films (Table 1). Root-mean-square roughness (Rq) refers to the mean size of peaks and valleys within the AFM images (Thomas, 1981; Wang *et al.* 2013). Pullulan films presented the lowest R_q values (0.182 nm) among the tested samples. Moreover, the R_q values increased significantly with increasing alginate content from 40 to 100%. A similar trend was observed in average roughness (R_a) values for pullulan–alginate-based films. These results implied that the addition of alginate improved the roughness of resulting films. As analyzed in the subsection Barrier Properties of the Section Results, we found that incorporating alginate into pullulan increased WVP and Po_2 values of films. Therefore, we speculated that surface roughness of pullulan–alginate-based films was an important parameter, which influences their barrier properties.

TABLE 1. ROUGHNESS PARAMETERS OBTAINED FROM ATOMIC FORCE MICROSCOPY ANALYSIS OF PULLULAN, ALGINATE AND BLEND FILMS

Film type	R_q (nm)	R_a (nm)
Pullulan	$0.182 \pm 0.006†^{a}$	0.146 ± 0.007^{a}
Pul : alg(60:40)	$2.95 \pm 0.13‡^{b}$	2.44 ± 0.15^{b}
Alginate	6.36 ± 0.91^{c}	5.22 ± 0.89^{c}

† Means of three replicates ± standard deviations.
‡ Values were expressed as the means and standard deviations of three measurements.
Superscripted letters (a–c) indicate significant ($P < 0.05$) difference within the same column.

CONCLUSION

In this study, we investigate the water vapor and oxygen permeability, and microstructure of pullulan, alginate and blend films. According to our results, pure pullulan films exhibited a lower WVP value compared with alginate films, while blend films presented over twice the WVP value of the pure pullulan films. A similar tendency was observed for oxygen permeability as well. This could be attributed to interactions that occurred between pullulan and alginate. Thus, the barrier properties of tested films demonstrated that pure pullulan films were more suitable for packaging solid beverage products compared with pure alginate films. In terms of the microstructure of the films, based on the FTIR analysis, oxygen atoms at the second and third positions of the pyranose ring for alginate might have hydrogen bonded with pullulan chains. Meanwhile, the crystalline structure of pullulan–alginate-based films was determined by XRD. Compared with pure alginate, the crystalline structure of blend films changed, i.e., the crystallinity degree decreased. From the AFM results, pure pullulan films exhibited a smooth morphology with very small dust particles, while pure alginate displayed a textured surface consisting of packed grain-like particles. Considering the figures of WVP and Po_2 for pullulan–alginate-based films, it could be concluded that the barrier properties of tested films are positively correlated to their surface roughness.

ACKNOWLEDGMENTS

The authors gratefully acknowledge the Young Scholars Program from the Department of Science and Technology from Hunan Province (13B048). In addition, we would like to thank Dr. Loong-Tak Lim from the University of Guelph (Guelph, Canada) for the oxygen permeability measurement.

REFERENCES

ASTM. 1993. *Annual Book of ASTM Standards*, p. 593, American Society for Testing & Materials, Philadelphia, PA.

ASTM. 1995. *Annual Book of ASTM Standards*, American Society for Testing & Materials, Philadelphia, PA.

AZEREDO, H.M.C., MAGALHAES, U.S., OLIVEIRA, S.A., RIBEIRO, H.L., BRITO, E.S. and DE MOURA, M.R. 2012. Tensile and water vapour properties of calcium-crosslinked alginate–cashew tree gum films. Int. J. Food Sci. Technol. *47*, 710–715.

CAYKARA, T., DEMIRCI, S., EROĞLU, M.S. and GUVEN, O. 2005. Poly (ethylene oxide) and its blends with sodium alginate. Polymer *46*, 10750–10757.

FABRA, M.J., JIMENEZ, A., ATARE´S, L., TALENS, P. and CHIRALT, A. 2009. Effect of fatty acids and beeswax addition on properties of sodium caseinate dispersions and films. Biomacromolecules *10*, 1500–1507.

FU, S., THACKER, A., SPERGER, D.M., BONI, R.L., BUCKNER, I.S., VELANKAR, S., MUNSON, E.J. and BLOCK, L.H. 2011. Relevance of rheological properties of sodium alginate in solution to calcium alginate gel properties. AAPS PharmSciTech *12*, 453–460.

GALUS, S. and LENART, A. 2013. Development and characterization of composite edible films based on sodium alginate and pectin. J. Food Eng. *115*, 459–465.

GENNADIOS, A., WELLER, C.L., HANNA, M.A. and FRONING, G.W. 1996. Mechanical and barrier properties of egg albumen films. J. Food Sci. *61*, 585–589.

GIANCONE, T., TORRIERI, E., PIERRO, P.D., MARINIELLO, L., MORESI, M., PORTA, R. and MASI, P. 2008. Role of constituents on the network formation of hydrocolloid edible films. J. Food Eng. *89*, 195–203.

GOMEZ-ORDOÑEZ, E. and RUPEREZ, P. 2011. FTIR-ATR spectroscopy as a tool for polysaccharide identification in edible brown and red seaweeds. Food Hydrocolloids *25*, 1514–1520.

HUQ, T., SALMIERI, S., KHAN, A., KHAN, R.A., LE TIEN, C., RIEDL, B., FRASCHINI, C., BOUCHARD, J., URIBE-CALDERON, J., KAMAL, M.R., *et al.* 2012. Nanocrystalline cellulose (NCC) reinforced alginate based biodegradable nanocomposite film. Carbohydr. Poly. *90*, 1757–1763.

LACROIX, M. and LE TIEN, C. 2005. Edible films and coatings from non-starch polysaccharides. In *Innovations in Food Packaging*, (J.H. Han, ed.) pp. 338–361, Elsevier Academic Press, London, UK.

LEAL, D., MATSUHIRO, B., ROSSI, M. and CARUSO, F. 2008. FT-IR spectra of alginic acid block fractions in three species of brown seaweeds. Carbohydr. Res. *343*, 308–316.

LI, Y., JIA, H., CHENG, Q., PAN, F. and JIANG, Z. 2011. Sodium alginate–gelatin polyelectrolyte complex membranes with both high water vapor permeance and high permselectivity. J. Memb. Sci. *375*, 304–312.

ROJAS-GRAU, M.A., AVENA-BUSTILLOS, R.J., OLSEN, C., FRIEDMAN, M., HENIKA, P.R., MARTIN-BELLOSO, O., PAN, Z. and MCHUGH, T.H. 2007. Effects of plant essential oils and oil compounds on mechanical, barrier and antimicrobial properties of alginate–apple puree edible films. J. Food Eng. *81*, 634–641.

SAKATA, Y. and OTSUKA, M. 2009. Evaluation of relationship between molecular behaviour and mechanical strength of pullulan films. Int. J. Pharm. *374*, 33–38.

SALOMONSEN, T., JENSEN, H.M., STENBÆK, D. and ENGELSEN, S.B. 2008. Chemometric prediction of alginate monomer composition: A comparative spectroscopic study using IR, Raman, NIR and NMR. Carbohydr. Poly. *72*, 730–739.

SHIH, F., DAIGLE, K. and CHAMPAGNE, E. 2011. Effect of rice wax on water vapour permeability and sorption properties of edible pullulan films. Food Chem. *127*, 118–121.

SHINGEL, K.I. 2002. Determination of structural peculiarities of dexran, pullulan and γ-irradiated pullulan by Fourier-transform IR spectroscopy. Carbohydr. Res. *337*, 1445–1451.

SIEW, D.C.W., HEILMANN, C., EASTEAL, A.J. and COONEY, R.P. 1999. Solution and film properties of sodium caseinate/glycerol and sodium caseinate/polyethylene glycol edible coating systems. J. Agric. Food Chem. *47*, 3432–3440.

SINGH, R.S., SAINI, G.K. and KENNEDY, J.F. 2008. Pullulan: Microbial sources, production and applications. Carbohydr. Poly. *73*, 515–531.

SIRVIO, J.A., KOLEHMAINEN, A., LIIMATAINEN, H., NIINIMAKI, J. and HORMI, O.E.O. 2014. Biocomposite cellulose-alginate films: Promising packaging materials. Food Chem. *151*, 343–351.

SKJAK-BRÆK, G., MOE, S., SMIDSROD, O. and INGARDRAGET, K. 2006. Alginates. In *Food Polysaccharides and their Applications* (A.E. Stephen, G.O. Phillips and P.A. Williams, eds.) pp. 289–334, CRC Press, Boca Raton, FL.

THOMAS, T. 1981. Characterization of surface roughness. Precis. Eng. *3*, 97–104.

TROVATTI, E., FERNANDES, S.C.M., RUBATAT, L., PEREZ, D.D.S., FREIRE, C.S.R., SILVESTRE, A.J.D. and NETO, C.P. 2012. Pullulan–nanofibrillated cellulose composite films with improved thermal and mechanical properties. Compos. Sci. Technol. *72*, 1556–1561.

WANG, L.-J., YIN, Y.-C., YIN, S.-W., YANG, X.-Q., SHI, W.-J., TANG, C.-H. and WANG, J.-M. 2013. Development of novel zein-sodium caseinate nanoparticles (ZP)-stabilized emulsion films for improved water barrier properties via emulsion/solvent evaporation. J. Agric. Food Chem. *61*, 11089–11097.

XIAO, Q., LIM, L.-T. and TONG, Q. 2012. Properties of pullulan-based blend films as affected by alginate content and relative humidity. Carbohydr. Poly. *87*, 227–234.

YANG, G., ZHANG, L., PENG, T. and ZHONG, W. 2000. Effects of Ca^{2+} bridge cross-linking on structure and pervaporation of cellulose/alginate blend membranes. J. Memb. Sci. *175*, 53–60.

ZHANG, C., GAO, D., MA, Y. and ZHAO, X. 2013. Effect of gelatin addition on properties of pullulan films. J. Food Sci. *78*, C805–C810.

ZHONG, D., HUANG, X., YANG, H. and CHENG, R. 2010. New insights into viscosity abnormality of sodium alginate aqueous solution. Carbohydr. Poly. *81*, 948–952.